

# $\gamma$ -Ray Astronomy with MAGIC above 25 GeV

Thomas Schweizer\* for the MAGIC collaboration

\*Max-Planck-Institute for Physics, Föhringer Ring 6, 80805 Munich

**Abstract.** The MAGIC telescopes are 17 m diameter Cherenkov telescopes, located on the Canarian island La Palma (Spain), with an optimal view on the Northern sky. It is nowadays the only ground-based instrument able to measure high-energy  $\gamma$ -rays below 100 GeV. A recent upgrade of the trigger system allows to extend the sensitivity down to 25 GeV, which resulted in the detection of pulsed emission from the Crab pulsar. The construction of the second telescope MAGIC-II has been completed and commissioning is in its final phase. We review some recent experimental results obtained with the single telescope MAGIC-I.

**Keywords:**  $\gamma$ -ray MAGIC Cherenkov-telescope

## I. INTRODUCTION TO THE EXPERIMENT

The Major Atmospheric Gamma Imaging Cherenkov (MAGIC) telescopes are latest-generation instruments for very high energy (VHE)  $\gamma$ -ray observation exploiting the Imaging Air Cherenkov (IAC) technique. This kind of instrument images the Cherenkov light produced in the particle cascade initiated by a  $\gamma$ -ray in the atmosphere. Located at the Roque de los Muchachos Observatory, in La Palma (Spain), MAGIC incorporates a number of technological improvements in its design and achieves the lowest energy threshold (55 GeV with the nominal trigger, 25 GeV with the so-called analogue sum trigger [1], [2], [3], see Fig. 11) among instruments of its kind. MAGIC signal digitization uses 2 GSamples/s Flash Analog-to-Digital Converters. In the analysis we use time image parameters that take advantage of the sub-nanosecond timing precision of MAGIC readout [4], yielding a sensitivity (at a flux peak energy of 280 GeV) of 1.6% of the Crab Nebula flux in 50 hours of observations. The relative energy resolution above 200 GeV is better than 25%. The angular resolution is  $\sim 0.1^\circ$ , while source localization in the sky is provided with a precision of  $\sim 2'$ . MAGIC has the capability to operate under moderate illumination [5] (i.e. moon or twilight). This allows us to increase the duty cycle by a factor 1.3 and a better sampling of variable sources is possible.

The construction of a second telescope (MAGIC-II) has been completed and commissioning is in its final phase. Regular observations are scheduled for the beginning of October 2009. One special feature of both MAGIC telescopes is the light-weight construction of the telescope frame and after a recent upgrade of the drive system the telescope rotates by 180 degrees in less than 20 seconds. This is essential for the observation of  $\gamma$ -ray bursts.

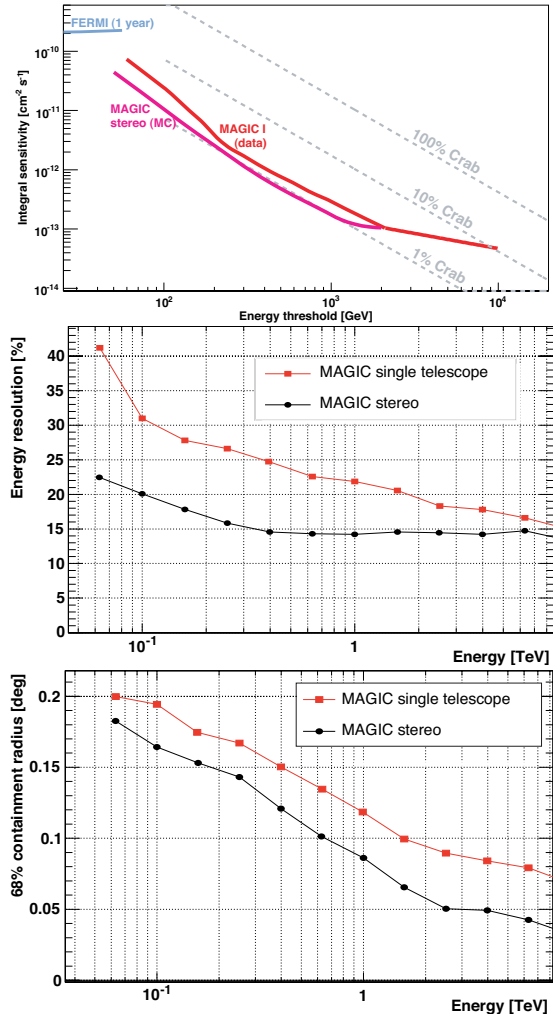


Fig. 1. Improvement in sensitivity (upper panel) and energy resolution as expected by MC studies in stereoscopic mode by using the second MAGIC telescope. The sensitivity will be around 1.0% of the Crab Nebula flux in 50 hours of observations in the core energy range of 200 GeV to 600 GeV. The energy resolution (middle panel) will be around 15%. Also the angular resolution (lower panel) in stereo mode will significantly improve compared to the single telescope mode.

Stereo observations will improve significantly the sensitivity of the single MAGIC telescope, the angular and the energy resolution (see Fig. 1).

MAGIC has been operating since fall 2004, carrying out a physics program which includes both, topics of fundamental physics and astrophysics. We highlight the latest MAGIC contributions to Extragalactic and Galactic astrophysics.

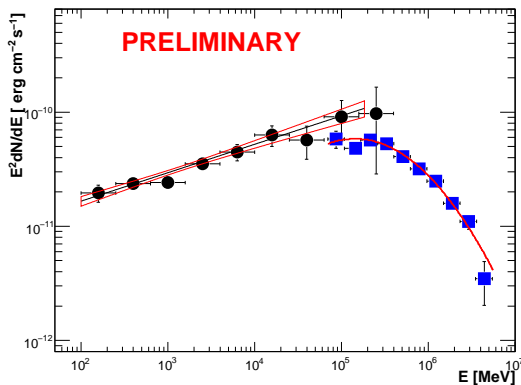


Fig. 2. Spectral energy distribution of the Mrk421 during the period Jan 20 2009 to April 27 2009 as measured by the Fermi-LAT (black circles) and MAGIC telescope (blue squares). The black line going over the Fermi data points is the resulting likelihood fit with a pure power law function, and the red contour is the 68% uncertainty of the fit. The red line going over the MAGIC data points is the result of a fit with a log-parabola function. Fermi and MAGIC spectra overlap in the energy range 80-400 GeV, where there is good agreement within the quoted statistical errors.

## II. EXTRAGALACTIC OBSERVATIONS WITH MAGIC

Most of the 28 currently known VHE  $\gamma$ -ray emitting AGNs [6] are high-frequency peaked BL Lac objects<sup>1</sup>.

AGN, in general, have a spectral energy distribution (SED) which is characterized by a second peak at very high  $\gamma$ -ray energies. In synchrotron-self-Compton (SSC) models this peak is assumed to be due to the inverse-Compton (IC) of electrons, by upscattering previously produced synchrotron photons to high energies. In external-Compton (EC) models also photons from other sources such as the accretion disc are upscattered to TeV energies. The previous model is used for most high frequency peaked BLLAC objects (HBLs) while for many low frequency peaked BLLACs (LBLs) the latter models describe the data more accurately.

In hadronic models, instead, interactions of a highly relativistic jet outflow with ambient matter, proton-induced cascades, or synchrotron radiation off protons, are the origin of the high-energy photons. Another defining property of blazars is the high variability of their emission ranging from radio to  $\gamma$ -rays. The  $\gamma$ -ray emission mechanism of radio galaxies and radio quasars are only poorly understood and still under discussion.

Time-resolved multi-wavelength observations are crucial for advanced understanding of AGN and the particle acceleration mechanism in the jets of those objects. Nowadays, instruments exist in wide ranges of the AGN energy spectrum and consequently, physics modeling of those sources will become much more realistic as the data is quite restrictive.

MAGIC is frequently participating in multi-wavelength campaigns. The energy range from MeV to GeV has been unobservable for many sources because

<sup>1</sup>See <http://www.mpp.mpg.de/~rwagner/sources/> for an up-to-date source list.

of too low fluxes which could not be detected by the EGRET satellite. This gap has now been closed by the space-borne HE Fermi  $\gamma$ -Ray Telescope (100 MeV-300 GeV). Fig. 2 shows the first multiwavelength spectrum of the full IC peak by observations of the Fermi  $\gamma$ -Ray Telescope and MAGIC [8]. The agreement between the Fermi spectrum and the MAGIC measurements is remarkable, given the fact that the Fermi data contains periods when MAGIC was not observing (daytime, moontime etc.). There might be still systematic uncertainties in the energy calibration.

MAGIC has observed 22 AGNs among which MAGIC has discovered 8 AGNs. Some of them are very interesting AGN objects as e.g. BLLAC. It is the prototype source, which all other BL Lac type AGN have been named after. BL Lac is the first discovered low frequency peaked BL Lac [9] object at VHE  $\gamma$ -ray energies.

For many of those VHE  $\gamma$ -ray blazars, correlations between X-ray and  $\gamma$ -ray emission have been found on time scales ranging from  $\sim 10$  minutes to days and months (see, e.g., [10], [11]). For others such as Mkn 180 [12], 1ES 1011+496 [13] and S50716+114 [14] also optical correlations seem possible. The latter will be described in more detail.

MAGIC has also observed the sky region of 3C 66A and 3C 66B. 3C 66A is a distant blazar at redshift  $z=0.44$ , while 3C 66B is a nearby FR-I radio galaxy. The observation was triggered by an optical outburst of 3C 66A [15]. VERITAS recently detected and has reported on 3C 66A [16]. As will be explained later on, the source detected by MAGIC is not coinciding with 3C 66A but rather with 3C 66B.

One of the most prominent MAGIC highlights is 3C 279, the first flat spectrum radio quasar, also discovered by MAGIC. It has the highest redshift of  $z = 0.536$  of all detected AGN so far [17]. The previous detection in 2006 was confirmed again in a follow-up observation in 2007 [18].

Another AGN presented here is M87. It is a very close-by giant radio galaxy. The observations presented here have been carried out in a multi-wavelength observation by MAGIC, VERITAS, H.E.S.S. on the one hand and VLBA radio imaging and monitoring by the X-ray satellite *Chandra* on the other.

One of the main extragalactic MAGIC targets that are not AGN are GRBs. A recent upgrade of the drive system allows MAGIC to point the telescopes within 20 seconds to any point in the sky, thus greatly enhancing the probability to catch a close-by burst. Bursts that last long enough and that are closer than a redshift of  $z = 1$  are believed to be detectable by MAGIC since the Fermi satellite has already detected single VHE  $\gamma$ -photons from two GRBs. Taking into account the high redshift of those GRBs ( $z = 4.3$  and  $z = 1.8$ ), the original energy of those  $\gamma$ -photons were about 70 GeV and 90 GeV, respectively. Such  $\gamma$ -energies are clearly within the detectable energy range of MAGIC [19], [20].

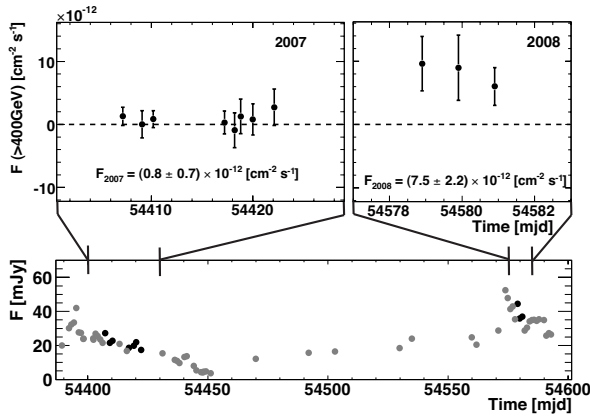


Fig. 3. The lightcurve of S5 0716+71. The upper two panels show the flux above 400 GeV as observed with MAGIC in the years 2007 and 2008. The lower panel shows the optical lightcurve as observed with the KVA telescope in La Palma. The days in which MAGIC observed this source are drawn in black.

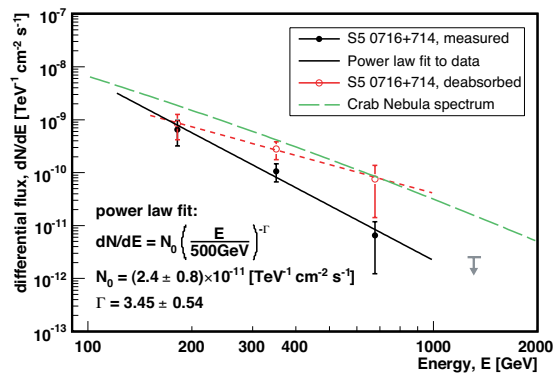


Fig. 4. The Spectrum of S5 0716+71 ( $z = 0.31$ ). The differential energy spectrum follows a powerlaw with a spectral index of  $\Gamma = 3.45 \pm 0.54_{stat} \pm 0.2_{syst}$  and an integral flux of  $F_{>400\text{GeV}} = (7.5 \pm 2.2_{stat} \pm 2.3_{syst}) \times 10^{-12} \text{cm}^{-2} \text{s}^{-1}$ .

#### A. Blazars Detected during Optical Outbursts

MAGIC has been performing target of opportunity observations upon high optical states of known or potential VHE blazars. Up to now, this strategy has proven rather successful with the discovery of Mkn 180 [12] and IES 1011+496 [13]. Recently also S5 0716+71 [14] was successfully detected at VHE  $\gamma$ -rays as third source by an optical target of opportunity trigger. So far, the detection efficiency of this strategy has been around 50%.

The 18.7 h observation of IES 1011+496 was triggered by an optical outburst in March 2007, resulting in a  $6.2\sigma$  detection above 200 GeV with an integrated flux of  $F_{>200\text{GeV}} = (1.58 \pm 0.32) \times 10^{-11} \text{cm}^{-2} \text{s}^{-1}$  [13]. An indication for an optical–VHE correlation is given, as in spring 2007 the VHE  $\gamma$ -ray flux is about 40% higher than in spring 2006, when MAGIC observed this blazar as part of a systematic search for VHE emission from a sample of X-ray bright ( $F_{1\text{keV}} > 2 \mu\text{Jy}$ ) HBLs [21].

The observations of S5 0716+71 were performed in November 2007 and April 2008 for a total live time

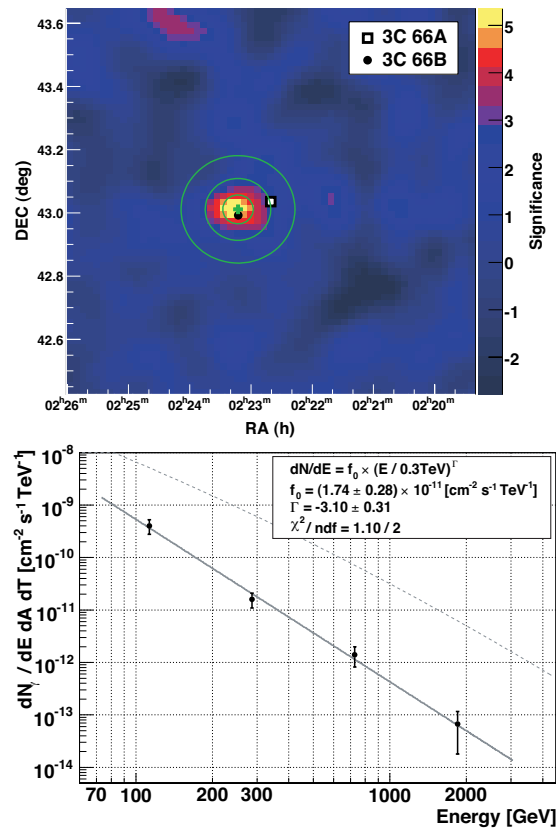


Fig. 5. The upper figure shows the location of the detected source MAGIC J0223+430 in the skymap of the 3C66 A/B region. The source seen corresponds clearly to object 3C 66B. The lower figure shows the spectrum of the observed object. The spectral index has a value of  $\Gamma = 3.10 \pm 0.31$ . The spectrum extends up to about 2 TeV.

of 13.1 hours. It was triggered in April 2008 by the KVA telescope in La Palma during an optical outburst April 17, 2008, where it reached its historical maximum value. The overall significance of the signal amounts to  $5.8\sigma$ . The observations in April 2008 were carried out at high zenith angle between 47 and 55 degrees for a live-time of 2.8 h, resulting in a strong  $6.8\sigma$  signal (Fig. 3). The differential energy spectrum follows a powerlaw with a spectral index of  $\Gamma = 3.45 \pm 0.54_{stat} \pm 0.2_{syst}$  and a spectral flux of  $F_{>400\text{GeV}} = (7.5 \pm 2.2_{stat} \pm 2.3_{syst}) \times 10^{-12} \text{cm}^{-2} \text{s}^{-1}$  [14] (Fig. 4). In this case, the indication for an optical–VHE correlation is given by the fact, that in April 2008, during the historical optical high state, the VHE  $\gamma$ -flux is about nine times higher than in November 2007. The determination of the before unknown redshift S5 0716+71 ( $z = 0.31$ , [22]) makes this object the third most distant TeV blazar after 3C 279.

Given these three cases, one can conclude that for some types of AGN a correlation between optical flux and  $\gamma$ -ray flux seems probable.

#### B. Observations of the 3C 66A/B region

The MAGIC telescope observed the region around the distant blazar 3C 66A and 3C 66B for 54.2 h in August–December 2007. 3C 66A is a distant blazar with

a possible redshift of  $z=0.44$  [15] and 3C 66B is a nearby FR-I radio galaxy. The observations were triggered by an optical outburst of 3C 66A and led to the discovery of a  $\gamma$ -ray source centered at the celestial coordinates  $RA = 2^h 23^m 12^s$  and  $DEC = 43^\circ 0'.7$  (MAGIC J0223+430, see Fig. 5). Interestingly, the location of this source does not coincide with 3C 66A, which has been recently detected by VERITAS [16], but with the nearby radio galaxy 3C 66B. The identification with 3C 66A is excluded at a confidence level of 85% including systematic pointing uncertainties of the telescope.

The energy spectrum of MAGIC J0223+430 follows a power law with a normalization of  $(1.7 \pm 0.3_{\text{stat}} \pm 0.6_{\text{syst}}) \times 10^{-11} \text{TeV}^{-1} \text{cm}^{-2} \text{s}^{-1}$  at 300 GeV and a photon index  $\Gamma = 3.10 \pm 0.31_{\text{stat}} \pm 0.2_{\text{syst}}$ . The spectral index of MAGIC J0223+430 is different from the spectral index of 3C 66A ( $\Gamma = 4.10 \pm 0.4$ ) as observed by VERITAS. Investigating the absorption of VHE  $\gamma$ -rays from MAGIC J0223+430 allows us to calculate an upper limit on the redshift of  $z < 0.17$  [23] under the assumption that the intrinsic spectrum cannot be harder than  $\Gamma = 1.5$ . This excludes 3C 66A as possible candidate for identification. In addition, the spectrum of MAGIC J0223+430 extends up to 2 TeV, which is only possible if the source has a low redshift.

Considering all these indications, we conclude 3C 66B as a possible source for the observed signal. However, a signal contribution of 3C 66A to MAGIC J0223+430 cannot be excluded, partially at low energies.

### C. Strong Flaring of Messier 87 in February 2008

The giant radio galaxy M87 has been known as VHE  $\gamma$ -ray emitter ([24] and refs. therein). It is also one of the best-studied AGN. To assess variability timescales and the location of the VHE engine in M87, the H.E.S.S., VERITAS, and MAGIC collaborations carried out a shared monitoring of M87, resulting in  $\approx 120$  h observations in 2008 [25]. Results from the entire campaign have been published in [26]. During the MAGIC observations, a strong  $8\sigma$  signal was found on February 1, 2008, triggering the other Cherenkov telescopes as well as *Swift* X-ray observations. For the first time, MAGIC determined the energy spectrum below 250 GeV [27], which can be described by a power law with a spectral index of  $\Gamma = 2.30 \pm 0.11_{\text{stat}} \pm 0.20_{\text{syst}}$ . We did not measure a high-energy cut-off, but found a marginal spectral hardening, which may be interpreted as a similarity to other blazars detected at VHE, where such hardening has often been observed [6].

Our analysis revealed a variable ( $5.6\sigma$ ) night-to-night  $\gamma$ -ray flux above 350 GeV, while no variability was found for 150–350 GeV [27]. This fast variability  $\Delta t$  observed so far with MAGIC in the TeV  $\gamma$ -energy range, confirms the  $E > 730$  GeV short-time variability reported earlier [24], is in the order of or even below one day, restricting the emission region to a size of  $R \leq \Delta t c \delta = 2.6 \times 10^{15} \text{cm} = 2.6 \delta$  Schwarzschild radii (Doppler factor  $\delta$ ), and suggests the core of M87

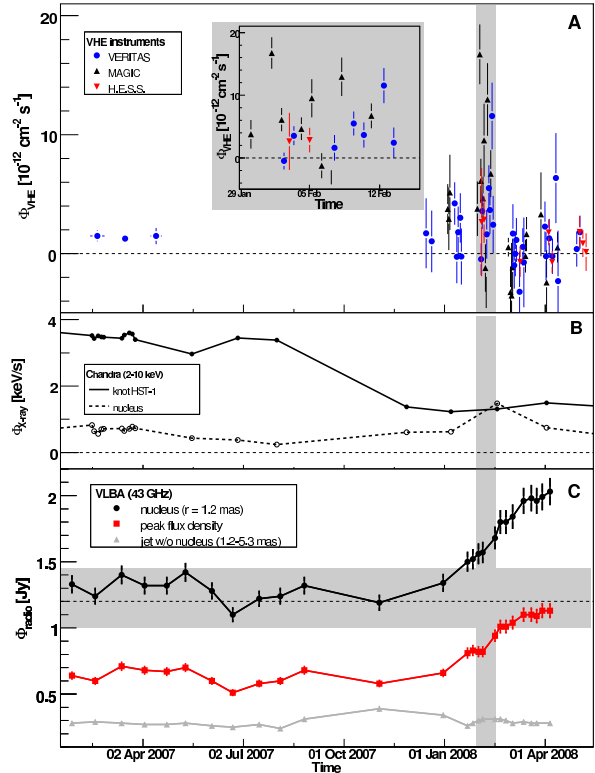


Fig. 6. Lightcurve of M87 in three wavebands from April 2007 until April 2008, including a  $\gamma$ -ray outburst on February 1, 2008. (A) shows the VHE  $\gamma$ -ray flux as observed by MAGIC, VERITAS and H.E.S.S.. (B) shows the X-ray flux of two different regions in the jet as observed by the *Chandra* X-ray satellite: (1) the nucleus of M87 and (2) the hot spot HST-1, the brightest spot observed by the Hubble space telescope. The lower panel (C) shows the radio flux as observed by VLBA (43GHz) imaging of three jet regions (1) The nucleus region (radius 1.2 mas), (2) the peak flux of the core (resolution element of  $0.21 \times 0.43$  mas or  $30 \times 60 R_S$ ) and (3) the jet without nucleus.

rather than the brightest known knot in the M87 jet, HST-1, as the origin of the TeV  $\gamma$ -rays. During the MAGIC observations HST-1 was at a historically low X-ray flux level, whereas at the same time the core luminosity reached a historical maximum [7].

During the MAGIC, VERITAS and H.E.S.S. observation campaign, M87 has been simultaneously monitored by the X-ray satellite *Chandra* and by VLBA imaging (at 43 GHz), both allowing a fine resolution of the jet and several hot spots close to the nucleus of M87 [26]. The lightcurves of the *Chandra* X-ray flux of the nucleus, the hot spot HST-1 and the VLBA radio flux of the nucleus and the close-by jet are shown in Fig. 6. It can be seen that the nucleus shows an increased X-ray flux during the VHE gamma-ray flare, while HST-1 is unchanged. Similarly, the VHE  $\gamma$ -ray outburst marks the beginning of a larger and longer-term radio flare of the nucleus and its surrounding region. The jet at larger distances ( $> 1.2$  mas or  $180 R_S$  away from the core) shows no variability. This suggests that the  $\gamma$ -ray emission happens just before the ejection of a new radio blob.

The combination of all these facts strongly support the core as the VHE  $\gamma$ -ray emission region of M87.

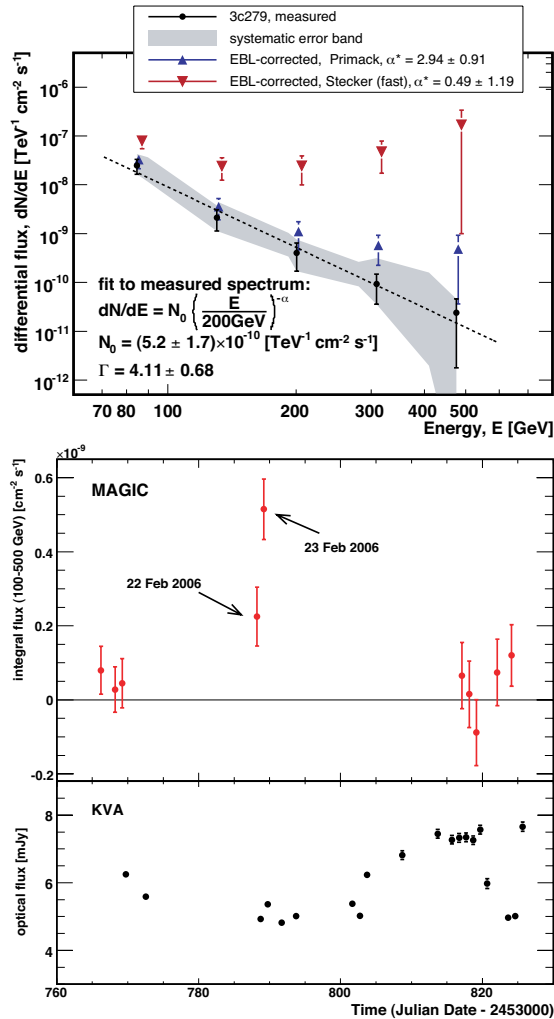


Fig. 7. Upper panel: Differential energy spectrum of 3C 279 in 2006. The grey area includes the combined statistical ( $1\sigma$ ) and systematic errors. The dotted line shows compatibility of the measured spectrum with a power law of photon index  $\alpha = 4.1$ . The triangles are measurements corrected on the basis of two models for the EBL density (see text). Lower panel: Lightcurve of the observation in 2006.

#### D. Detection of the flat-spectrum radio quasar 3C 279

Observations of 3C 279, the brightest EGRET AGN [28], revealed a  $5.77\sigma$  post-trial detection on February 23, 2006 supported by a marginal signal on the preceding night [29]. The overall probability for a zero-flux lightcurve can be rejected on the  $5.04\sigma$  level. Simultaneous optical  $R$ -band observations found 3C 279 in a high optical state, a factor of 2 above its long-term baseline flux, but with no indication of short time-scale variability. The observed VHE spectrum can be described by a power law with a photon spectral index of  $\Gamma = 4.1 \pm 0.7_{\text{stat}} \pm 0.2_{\text{syst}}$  between 75 and 500 GeV (Fig. 7). The measured integrated flux above 100 GeV on 23 February is  $(5.15 \pm 0.82_{\text{stat}} \pm 1.5_{\text{syst}}) \times 10^{-10}$  photons  $\text{cm}^{-2} \text{s}^{-1}$ .

VHE observations of sources as distant as 3C 279 ( $z = 0.536$ ) were, until recently, deemed impossible due to the expected strong attenuation of the  $\gamma$ -ray flux by

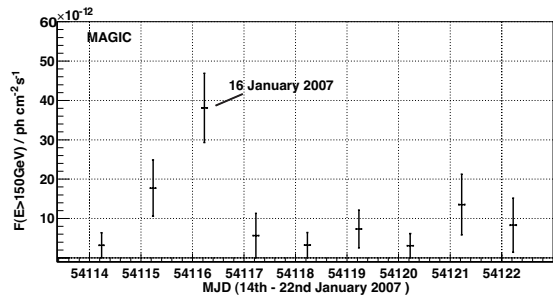


Fig. 8. This figure shows the lightcurve of 3C 279 during followup observations in January 2007. They reveal again a signal at the  $5.6\sigma$ -level on January 16, 2007.

the extragalactic background light (EBL), resulting in an exponential decrease with energy and a cutoff in the  $\gamma$ -ray spectrum. The observed VHE spectrum is sensitive to the EBL between  $0.2 - 2\mu\text{m}$ . The reconstructed intrinsic spectrum of the observations of 3C 279 in 2006 is difficult to reconcile with models predicting high EBL densities (e.g., the fast-evolution model of Stecker [30]), while low-level models, e.g. Primack [31], [32], are still viable. Assuming a maximum intrinsic photon index of  $\Gamma^* = 1.5$ , an upper EBL limit is inferred, leaving a small permissible region for the EBL.

The results support, at higher redshift, the conclusion drawn from earlier measurements [32] that the observations of the *Hubble Space Telescope* and *Spitzer* correctly estimate most of the light sources in the Universe thus leading to a rather low level EBL in the UV to near infrared.

The source has been re-observed in follow-up observations in January 2007, revealing again a detection on January 16, 2007 [18] at the  $5.6\sigma$ -level and thus confirming the previous detection. The lightcurve is shown in Fig. 8.

### III. GALACTIC OBSERVATIONS WITH MAGIC

MAGIC has observed many highly interesting galactic sources, such as the unidentified VHE  $\gamma$ -ray source TeV 2032+4130 [33], the shell type supernova remnants Cassiopeia A [34] and IC443 [36]. The latter will be described in more detail. MAGIC has also observed several binary systems such as Wolf-Rayet binaries [35], compact X-ray-binaries Cygnus X-1 [38], [37] and LSI+61 303 [39], [40], [41], which will be shown later on. Finally, one of our most prominent sources is the Crab nebula [43] from which we have detected pulsed radiation above 25 GeV. The detection of the Crab pulsar will be presented in greater detail.

#### A. Detection of pulsed emission above 25 GeV from Crab

The Crab Nebula is the standard candle for VHE astrophysics and therefore, a big fraction of MAGIC observation time is devoted to this object. A subsample of 16 hours of optimal data was used for measuring the energy spectrum of the nebula between 60 GeV and 8

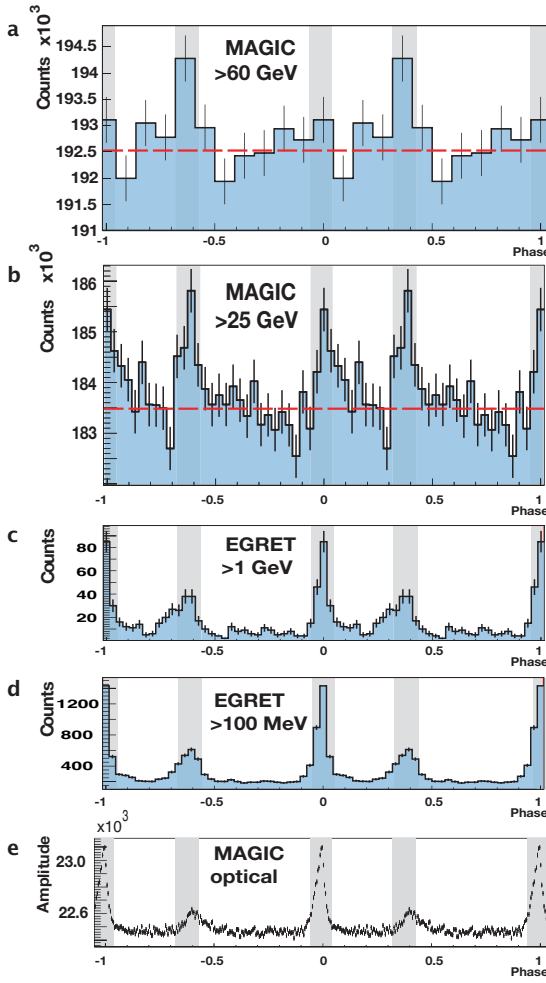


Fig. 9. The lightcurve of the Crab pulsar in several wavebands from top to bottom: (a) above 65 GeV by MAGIC, (b) above 25 GeV by MAGIC, (c) above 1 GeV by EGRET (d) above 100 MeV by EGRET and in the optical waveband by MAGIC.

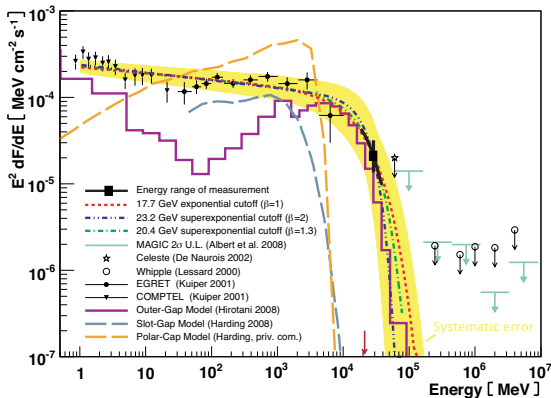


Fig. 10. The Crab pulsar's spectral cutoff. The black points and triangles on the left represent flux measurements from EGRET and COMPTEL. The cutoff was determined by simultaneously fitting power-law spectra with different exponential cutoffs to the measurements of MAGIC on the one hand, and EGRET and COMPTEL on the other hand. The fitted functions are compared with the most current pulsar models, a polar-cap model, a slot-gap model and an outer-gap model.

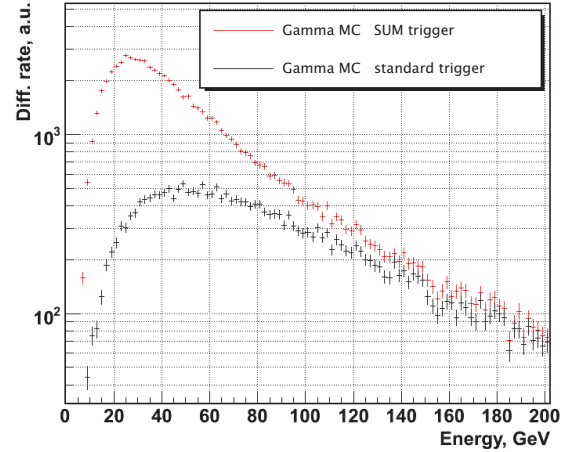


Fig. 11. The development of a new type of trigger, the so-called analogue sum trigger reduced the standard trigger threshold of 55-60 GeV down to about 25 GeV.

TeV [43]. The peak of the SED was measured at an energy  $E = (77 \pm 35)$  GeV. The VHE source is point-like and the position coincides with that of the pulsar.

In search for periodic signals from the nebula a periodicity analysis of those 16 h has been performed [43]. A hint of a periodic signal above 60 GeV has been seen at the  $2.9\sigma$  level [43]. This hint triggered activities to develop and install new type of trigger, the so-called analogue sum trigger, with a significantly lower trigger threshold at 25 GeV [1]. The standard trigger has a threshold of around 55-60 GeV (see Fig. 11).

New observations of the Crab pulsar from October 2007 to February 2008 using the new trigger setup led to the detection of pulsed VHE  $\gamma$ -ray emission above 25 GeV [1] at the  $6.4\sigma$ -level. The lightcurve of the Crab pulsar in several wavebands as observed by MAGIC and the EGRET detector, on board the Compton Gamma-Ray Observatory satellite, is shown in Fig. 9. The signal above 65 GeV in the second peak has a significance of  $3.4\sigma$ , which confirms the previous observation.

This result has revealed a relatively high energy cutoff  $E_{cut} = 17.7 \pm 2.8_{stat} \pm 5.0_{syst}$  GeV (see Fig. 10), indicating that the emission occurs far out, higher than  $r/R_{neutron} = 6.2 \pm 0.2_{stat} \pm 0.4_{syst}$  neutron star radii, in the magnetosphere, hence excluding the polar-cap scenario as a plausible explanation for the high-energy origin. This is also the first time that a pulsed  $\gamma$ -ray emission has been detected from a ground-based telescope, and it opens up the possibility of a detailed study of the pulsar's energy cutoff, which will help elucidate the mechanism of high energy radiation in these objects. More details can be found at [2].

### B. Compact binary LS I +61 303

LS I+61 303 is a very peculiar binary system containing a Be main-sequence star together with a compact object (neutron star or black hole), which displays periodic emission throughout the spectrum from radio

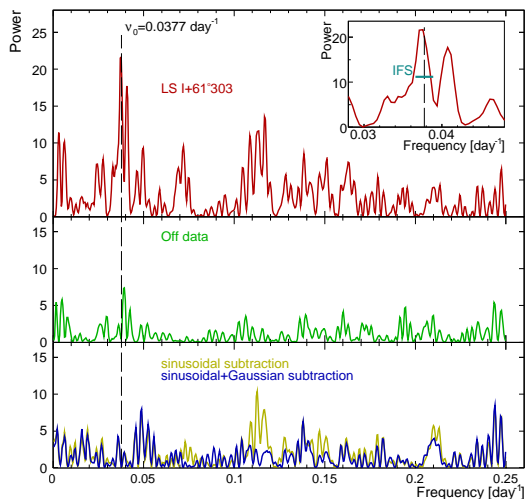


Fig. 12. Left: Lomb-Scargle periodogram for LSI+61 303 data (upper panel) and simultaneous background data (middle panel). In the lower panel we show the periodograms after subtraction of a sinusoidal signal at the orbital period (light line) and a sinusoidal plus a Gaussian wave form (dark line). The vertical dashed line corresponds to the orbital frequency. Inset: zoom around the highest peak, which corresponds to the orbital frequency ( $0.0377\text{d}^{-1}$ ). Its post-trial probability is  $\sim 10^{-7}$ . The IFS is also shown.

to X-ray wavelengths. Observations with MAGIC have determined that this object produces  $\gamma$ -rays up to at least  $\sim 4$  TeV [39], and that the emission is periodically modulated by the orbital motion ( $P_{TeV} = (26.8 \pm 0.2)\text{d}$ ) [40] (see Figure 12). The peak of the emission is always found at orbital phases around 0.6–0.7. During December 2006 we detected a secondary peak at phase 0.8–0.9. Between October and November 2006, we set up a multiwavelength campaign involving radio (VLBA, e-EVN, MERLIN), X-ray (*Chandra*) and TeV (MAGIC) observations [41]. Furthermore, we conducted a strictly simultaneous MW campaign with XMM, *Swift*, and MAGIC in September 2007. This campaign revealed strong evidence for a correlation between the X-ray and VHE  $\gamma$ -ray emission. No correlation is found between radio, VHE and  $\gamma$ -rays [42].

### C. Hadronic acceleration in the SNR IC 443?

We detected a new source of VHE  $\gamma$ -rays located close to the Galactic Plane, namely MAGIC J0616+225 [36], which is spatially coincident with the SNR IC 443. The measured energy spectrum is well fitted ( $\chi^2/n.d.f = 1.1$ ) by the following power law:  $(1.0 \pm 0.2) \times 10^{-11} (E/0.4\text{ TeV})^{-3.1 \pm 0.3} \text{TeV}^{-1} \text{cm}^{-2} \text{s}^{-1}$ .

MAGIC J0616+225 is point-like for MAGIC spatial resolution, and appears displaced to the south of the center of the SNR shell. It is spatially correlated with a molecular cloud [44] (see Fig. 13). There is also an EGRET source centered in the shell of the supernova remnant. The observed VHE radiation may be due to  $\pi^0$ -decays from interactions between cosmic rays accelerated in IC 443 and the dense molecular cloud. A

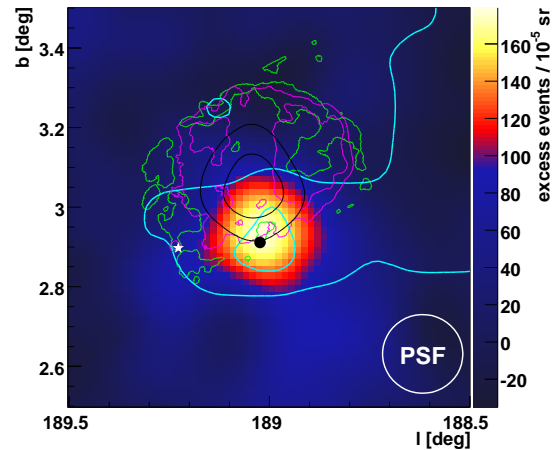


Fig. 13. MAGIC Skymap of IC 443. Overlaid are the CO emission lines (cyan) from Dame et al. (2001), contours of 20cm VLA radio data from Condon et al. (1998) (green), X-ray contours from Rosat (Asaoka & Aschenbach 1994) (purple) and  $\gamma$ -ray contours from EGRET (Hartmann et al. 1999) (black). The white star denotes the position of the pulsar CXOU J061705.3+222127 (Olbert et al. 2001). The black dot shows the position of the 1270 Mhz OH-maser (Claussen et al. 1997). The white circle is the MAGIC PSF.

possible distance of this cloud from IC 443 could explain the steepness of the measured VHE  $\gamma$ -ray spectrum. If the particle population were accelerated at the SNR Shock front a harder spectrum could be expected. Also, MAGIC J0616+225 is spatially correlated with maser emission (black dot in figure) [45]. Maser emission is an indication for a shock in a high matter density environment. These facts hint to a possible hadronic origin of the VHE  $\gamma$ -emission.

### IV. STATUS OF MAGIC II COMMISSIONING

The commissioning of the second telescope is almost completed. Regular stereoscopic observations are expected to start beginning of October 2009. All systems and hardware have been installed on-site and are working as expected. The telescope structure of MAGIC II is basically a clone of MAGIC I, while the camera and the read-out systems are new developments. Details of the hardware are described in [46]. Since the beginning of July 2009, the second telescope has already taken data in parallel with MAGIC I to check the stability of the system and to discover hidden problems. Figs. 14 and 15 show the first stereo signal obtained from the Crab nebula at high zenith angle ( $> 45$  degrees) and a typical  $\gamma$ -like shower recorded by both telescopes.

### ACKNOWLEDGMENTS

We thank the Instituto de Astrofísica de Canarias for the excellent working conditions at the Observatorio del Roque de los Muchachos in La Palma. The support of the German BMBF and MPG, the Italian INFN and Spanish MICINN is gratefully acknowledged. This work was supported by ETH Research Grant TH 34/043, by the polish MNiSzW Grant NN203 390834, and by the YIP of the Helmholtz Gemeinschaft.

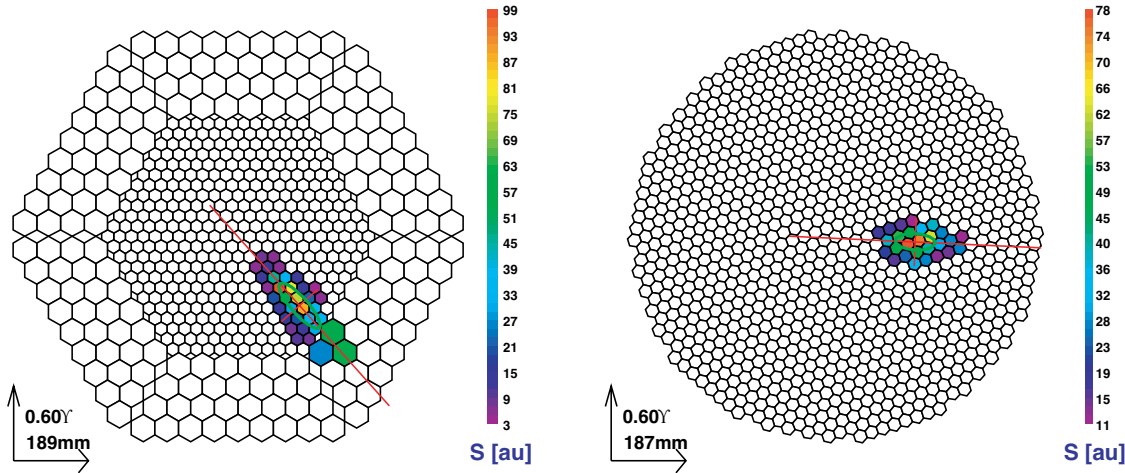


Fig. 14. The figure shows a typical  $\gamma$ -like event as seen simultaneously with MAGIC I and MAGIC II.

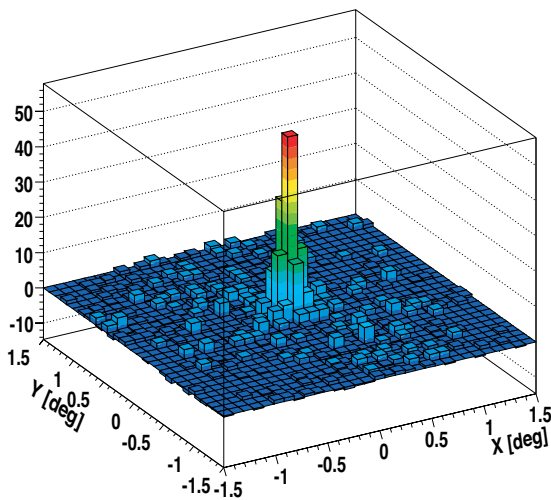


Fig. 15. The figure shows the first observed signal of the Crab nebula that has been recorded with both MAGIC telescopes in stereoscopic mode. The pointing accuracy is very good and the signal is concentrated in a small region only, even though the analysis performed is very basic and preliminary. The signal shows that the MAGIC telescopes are working as expected.

## V. AUTHOR INFORMATION

E-mail:tschweiz@mppmu.mpg.de

## REFERENCES

- [1] E. Aliu *et al.* (MAGIC Coll.) 2008, *Science* 322, 1221
- [2] M. Rissi, N. Otte, T. Schweizer, M. Shayduk, 2008, *Nuclear Science Symposium Conference Record, NSS '08. IEEE 19-25 Oct. 2008*, 1472 - 1475
- [3] M. Rissi, N. Otte, T. Schweizer, M. Shayduk, 2009, *Accepted for publication in TNS*
- [4] E. Aliu *et al.* (MAGIC Coll.) 2009, *Astropart. Phys.*, 30, 293.
- [5] Daniel Britzger *et al.* 2009, *proceedings, 31st ICRC Lodz 2009*, icrc 1269
- [6] R. M. Wagner 2008, *Mon. Not. R. Astr. Soc.*, 385, 119.
- [7] D. Harris, *priv. comm.*
- [8] D. Paneque *et al.* 2009, *Proceedings of "ACCRETION AND EJECTION IN AGN: A GLOBAL VIEW"*, Como, Italy.
- [9] J. Albert *et al.* 2007, *ApJ Lett.* 666, L17
- [10] G. Fossati *et al.* 2008, *Astrophys. J.*, 677, 906.
- [11] R. M. Wagner 2008, *PoS(BLAZARS2008)* 013.
- [12] J. Albert *et al.* (MAGIC Coll.) 2006, *Astrophys. J.*, 648, L105.
- [13] J. Albert *et al.* (MAGIC Coll.) 2007, *Astrophys. J.*, 667, L21.
- [14] H. Anderhub *et al.* (MAGIC Coll.) 2009, *submitted to Astrophys. Lett.*
- [15] E. Aliu *et al.* (MAGIC Coll.) 2009, *Astrophys. J.*, 692, L29.
- [16] V. A. Acciari, *et al.* 2009, *Astrophys. Lett.*, 693, L104.
- [17] MAGIC collaboration, 2008, *Science*, 320, 1752.
- [18] Karsten Berger *et al.* (MAGIC coll.) 2009, *Proceed. 31. ICRC Lodz.*, icrc 3C279.
- [19] A. A. *et al.* 2009, *Science*, 323, 1688.
- [20] Gamma ray burst circular network GCN 9867 (GRB 090902B) 2009, <http://gcn.gsfc.nasa.gov/gcn3/9867.gcn3>.
- [21] J. Albert *et al.* (MAGIC Coll.) 2008, *Astrophys. J.*, 681, 944.
- [22] K. Nilsson, T. Pursimo, A. Sillanpää, L. O. Takalo, E. Lindfors 2008, *Astron. Astrophys.*, 487, L29.
- [23] D. Mazin and M. Raue 2007, *A & A.*, 471, 439.
- [24] F. Aharonian *et al.* (H.E.S.S. Coll.) 2006, *Science*, 314, 1424.
- [25] M. Beilicke, M. Hui, D. Mazin, M. Raue, R. M. Wagner, S. Wagner (H.E.S.S., MAGIC, VERITAS Coll.) 2008 *in: Proc. Int. Symposium on High Energy Gamma-Ray Astron.*, Heidelberg, Germany.
- [26] The VERITAS Collaboration, The VLBA 43 GHz M 87 Monitoring Team, The H.E.S.S. Collaboration, The MAGIC Collaboration, 2009, *Science*, 325, 444-448.
- [27] J. Albert *et al.* (MAGIC Coll.) 2008, *Astrophys. J.*, 685, L23.
- [28] A. E. Wehrle *et al.* 1998, *Astrophys. J.*, 497, 178.
- [29] J. Albert *et al.* (MAGIC Coll.) 2008, *Science*, 320, 1752.
- [30] F. W. Stecker *et al.* 2007, *Astrophys. J.*, 667, L29.
- [31] J. R. Primack *et al.* 2005, *AIP Conf. Proc.*, 745, 23.
- [32] F. Aharonian *et al.* (H.E.S.S. Coll.) 2006, *Nature*, 440, 1018.
- [33] J. Albert *et al.* (MAGIC Coll.) 2008, *Astrophys. J.* 675, L25
- [34] J. Albert *et al.* (MAGIC Coll.) 2007, *A&A* 474, 937.
- [35] E. Aliu *et al.* (MAGIC Coll.) 2008, *Astrophys. J.* 685, L71
- [36] J. Albert *et al.* (MAGIC Coll.) 2007, *Astrophys. J.* 664, L87.
- [37] J. Rico 2008, *Astrophys. J.* 683, L55
- [38] J. Albert *et al.* (MAGIC Coll.) 2007, *Astrophys. J.* 665, L51.
- [39] J. Albert *et al.* (MAGIC Coll.) 2006, *Science* 312, 1771.
- [40] J. Albert *et al.* (MAGIC Coll.) 2008, *Astrophys. J.* in press, arXiv:0806.1865 [astro-ph]
- [41] J. Albert *et al.* (MAGIC Coll.) 2008 *Astrophys. J.* 684, 1351
- [42] Tobias Jogler *et al.* 2009, *proceedings, 31st ICRC Lodz 2009*, icrc 1161
- [43] J. Albert *et al.* (MAGIC Coll.) 2008, *Astrophys. J.* 674, 1037
- [44] R. H. Cornett, G. Chin G & G. R. Knapp 1977, *A&A* 54, 889
- [45] M. J. Claussens *et al.* 1997, *Astrophys. J.* 489, 143
- [46] Thomas Schweizer *et al.* (MAGIC coll.) 2009, *Proceed. 31. ICRC Lodz.*, icrc0342.